Chapter 5
Temperature Programmed Reduction/Oxidation (TPR/TPO) Methods

Antonella Gervasini

Abstract The redox properties of the metal oxides impart them peculiar catalytic activity which is exploited in reactions of oxidation and reduction of high applicative importance. It is possible to measure the extent of oxidation/reduction of given metal oxide by thermal methods which are become very popular: TPR and TPO analyses. By successive experiments of reduction and oxidation (TPR-TPO cycles) it is possible to control the reversible redox ability of a given oxide in view of its use as catalyst. The two methods are here presented with explanation on some possibility of exploitation of kinetic study to derive quantitative information on the reduction/oxidation of the oxide. Examples of selected metal oxides with well-established redox properties which have been used in catalytic processes are shown.

5.1 Redox Properties of Metal Oxides and Catalytic Implications

The important properties of metal oxides that are of certain interest in different fields of applied science and technology are connected with magnetic, electrical, dielectric, optical, acid-base, and redox behavior. In particular, transition metal oxides with redox properties are of interest for applications in catalysis [1]. Metal oxides and in particular transition metal oxides can possess more than one stable oxidation state making them possible to catalyze reactions which necessitate electron exchanges between reactant(s) and surface active sites (e.g., oxidation, dehydrogenation, etc.). Conversely, other kinds of metal oxides are known to be almost complete irreducible. Oxides of copper, nickel, cobalt, molybdenum, are only few examples of reducible

A. Gervasini (✉)
Dipartimento di Chimica,
Università degli Studi di Milano,
Via Camillo Golgi, Milan, Italy
e-mail: antonella.gervasini@unimi.it

A. Auroux (ed.), *Calorimetry and Thermal Methods in Catalysis*,
Springer Series in Materials Science 154, DOI: 10.1007/978-3-642-11954-5_5,

oxides and oxides of gallium or niobium are examples of *quasi*-irreducible oxides (for Ga_2O_3, any reduction is not observed up to 1000 °C and for Nb_2O_5, less than 50 % of Nb(V) can be reduced to Nb(IV) at temperature higher than 900 °C).

The reducing properties of metal oxides can be quantitatively established evaluating the reaction between the metal oxide (MO) and hydrogen to form metal (M) and water vapor:

$$MO_{(s)} + H_{2(g)} \rightarrow M_{(s)} + H_2O_{(g)} \tag{5.1}$$

The standard free energy change for the reduction (ΔG°) is negative for a number of oxides, thus indicating that for these oxides the reactions are thermodynamically feasible (Fig. 5.1). However, it may still possible for the reduction to proceed even when ΔG° is moderately positive. The following equation:

$$\Delta G = \Delta G^\circ + RT \ln (P_{H2O}/P_{H2}) \tag{5.2}$$

where P_{H2O} and P_{H2} denote partial pressures of water and hydrogen, respectively, has to be considered. If the experimental method of performing the reductions is that the water vapor is constantly swept from the reaction zone as it is formed, then P_{H2O} is lowered and it is possible that the term RT ln (P_{H2O}/P_{H2}) could be sufficiently negative to nullify the positive ΔG° value. This is likely to occur at high temperatures where it is possible to observe reduction phenomena for the oxides of vanadium, tin, chromium, which have positive ΔG° values in the range 40–100 kJ/mol (Fig. 5.1).

During some reactions catalyzed by metal oxides, they undergo reduction and reoxidation simultaneously by loss and gain of surface lattice oxygen to and from the gas phase. This phenomenon is called *redox catalysis.* The redox property as well as the acidic and basic feature is the most important properties of metal oxide catalysts. Some simple metal oxides, like V_2O_5, CoO_2, NiO, MnO_2, CeO_2, MgO and some mixed metal oxides have redox properties and they found application as they are or supported on ceramic carriers as oxidation catalysts.

The use of oxides and mixed metal oxides as heterogeneous catalysts in selective oxidation reactions, in particular, is of great industrial importance. In selective oxidation reactions, organic feeds are converted to useful products by oxygen insertion without any change of the number of carbons. The major processes include allylic oxidation (i.e., selective oxidation of olefins at the allylic position) to give aldehydes, nitriles, and acids; aromatic oxidation to acids and anhydrides, epoxidation to olefins, methanol oxidation to formaldehyde, etc. [3]. The desired selective oxidation reactions are, of course, thermodynamically favorable and the oxide catalysts are necessary to overcome kinetic limitations. Moreover, they have to select the desired oxidized product limiting the formation of the more thermodynamically favored deep oxidation products, like CO_2, H_2O, and HCN (Table 5.1 [3]).

The research and study of selective oxidation oxide catalysts with developed redox properties began more than five decades ago with the concept that the lattice oxygen of a reducible metal oxide could serve as a more versatile and useful oxidizing agent for hydrocarbons than would gaseous molecular oxygen. The role of molecular oxygen is only to replenish lattice oxygen vacancies and therefore an oxidation-

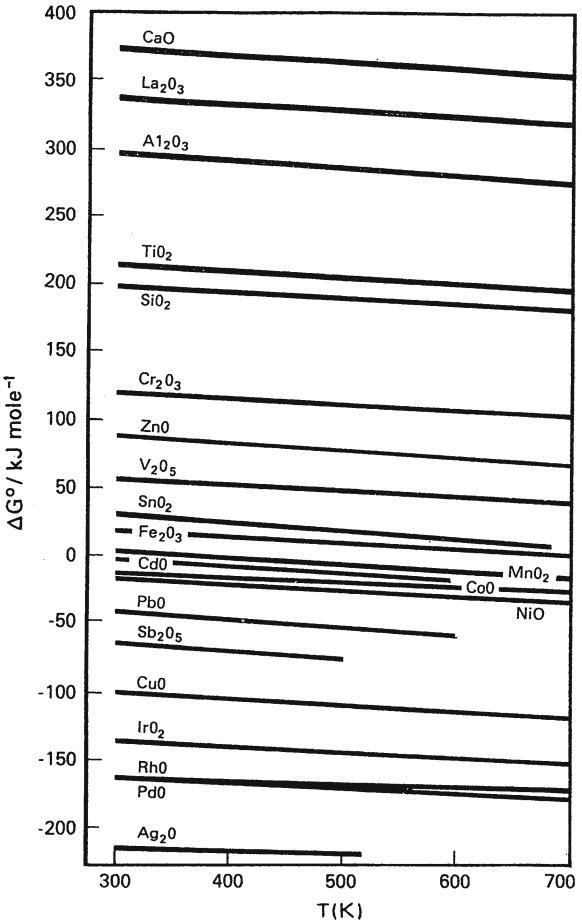

Fig. 5.1 Standard free energy change as a function of temperature (from Ref. [2])

Table 5.1 Thermodynamics of several selective and total oxidation reactions

	Reactions	$\Delta G^{\circ}_{427^{\circ}C}$(kcal/mol)
(A)	$C_3H_6 + O_2 \rightarrow CH_2 = CHCHO + H_2O$	− 80.82
(B)	$C_3H_6 + \frac{3}{2}O_2 \rightarrow CH_2 = CHCOOH + H_2O$	−131.42
(C)	$C_3H_6 + 3O_2 \rightarrow 3CO + 3H_2O$	−304.95
(D)	$C_3H_6 + \frac{9}{2}O_2 \rightarrow 3CO_2 + 3H_2O$	−463.86
(E)	$C_3H_6 + NH_3 + \frac{3}{2}O_2 \rightarrow CH_2 = CHCN + 3H_2O$	−136.09
(F)	$C_3H_6 + \frac{3}{2}NH_3 + \frac{3}{2}O_2 \rightarrow \frac{3}{2}CH_3CN + 3H_2O$	−142.31
(G)	$C_3H_6 + 3NH_3 + 3O_2 \rightarrow 3HCN + 6H_2O$	−273.48

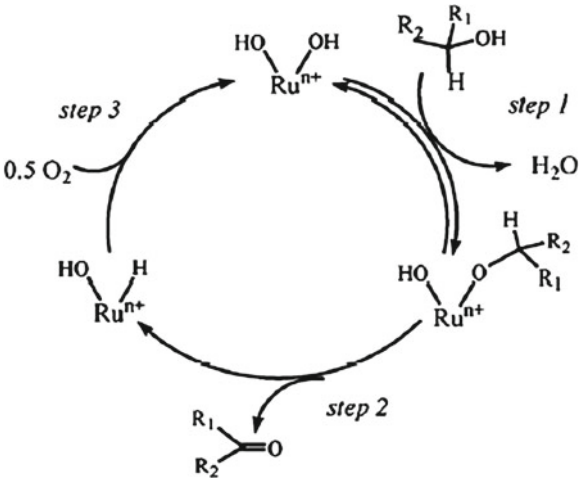

Fig. 5.2 Scheme of a catalytic selective oxidation-reduction cycle (from Ref. [3])

reductant cycle is recognized to hold in the selective catalytic oxidations (Fig. 5.2). Confirmation of the involvement of lattice oxygen in selective oxidation reaction (i.e., propylene oxidation) comes from experiments with $^{18}O_2$ as a vapor phase oxidant. From a mechanistic standpoint, reoxidation of the catalyst involves two processes: adsorption and activation of dioxygen and its incorporation into the solid vacancies (i.e., transformation of O_2 to O^{2-}).

This step requires electron transfer from the lattice to activate and dissociate the dioxygen before incorporation into the vacancies. When the oxygen vacancies are located near the surface, the reoxidation is very fast and activation energy for this surface vacancy reoxidation of the order of 5–10 kJ/mol. Reoxidation of subsurface vacancies is much slower and it is limited by the ability of the catalyst to transport the oxygen from the surface O_2-chemisorption sites to the subsurface vacancies. For example, γ-bismuth molybdate with its layer structure results in low-energy pathway for diffusion of the oxygen anions and reoxidation proceeds with an activation energy of only 35–38 kJ/mol. In more closed packed structures, like α-bismuth molybdate, rapid diffusion cannot occur and the reoxidation rate is diffusion limited with activation energy as high as 105–110 kJ/mol. Moreover, the presence of a redox couple in a catalyst can create a lower energy pathway for diffusion by promoting electron and oxygen transfer between the surface and the bulk. Incorporation of iron (Fe^{3+}/Fe^{2+} redox couple) into the α-bismuth molybdate structure, single $Bi_3FeMo_2O_{12}$ phase is formed, decreases the activation energy for the reoxidation process to 29–35 kJ/mol.

The real breakthrough in the appreciation of the idea of lattice oxygen depletion and subsequent replenishment governing the selective oxidation reactions took place after the appearance of a series of papers by Mars and Van Krevelen (MvK), in 1954 [4] describing some applications of their idea in the kinetics (Fig. 5.3). However,

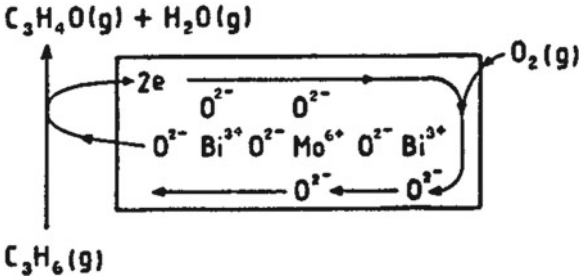

Fig. 5.3 Conversion of propylene into acroleine on bismuth molybdate following the Mars and Van Krevelen mechanism (from Ref. [4])

all oxidations are redox reactions, even when the prevailing mechanism can not be called a MVK mechanism

A property of key importance for an efficient selective oxidation catalyst is its tendency to donate the structural oxygens. If reduction of the catalyst is too facile, it may be well active but it ceases to be selective. Although the reoxidation rate is usually not rate determining in the overall redox cycle, the catalyst ability to replenish its reservoir of lattice oxygen is of fundamental importance in order to sustain the catalyzed reaction. While reoxidation at higher temperatures is generally fast for all the selective oxidation catalysts, it becomes more difficult at low temperatures, where selectivities to the usual products are highest.

Examples of reactions of industrial and environmental importance that run according MvK mechanism are alcohol selective oxidations, VOC total oxidations, selective catalytic reductions of NO_x by ammonia or hydrocarbons, and more recently photocatalytic oxidation of hydrocarbons [5] etc. Revisitation of MvK mechanism for various reactions appeared in Ref. [6] For each one of these reactions, a metal oxide-based catalyst with well-developed redox properties has been optimized.

The redox property of any metal oxide catalyst can be characterized by using the techniques of temperature-programmed reduction/temperature programmed oxidation (TPR/TPO). TPR is a relatively new technique used for the chemical characterization of solid materials. Since the first publications in this area (1975–1985), many papers have appeared in the literature showing TPR applicability in a variety of scientific fields, most particularly in characterization of catalysts. In 1982 the first review on the subject of TPR appeared in the literature [2]. TPR technique is based on the reducibility of species in/on solids by a gas, in general by hydrogen, at the same time that the temperature of the system is changed in a predetermined way (in general, linear temperature increase). The decrease in reducing gas concentration in the effluent gas with respect to its initial concentration allows monitoring the reduction progress. The obtained results enable obtaining information not only of a purely analytical nature but also, and more importantly, about the condition of species present in/on solids. The technique is relatively simple in concept and application and as a result, TPR and related techniques are becoming commonly used among catalysis scientists.

More recently, combination of TPR technique with the temperature programmed oxidation technique (TPO) is imposing in the catalyst characterization studies [7]. In TPO, the catalyst is in the reduced form and is submitted to a programmed temperature increase, while an oxidizing mixture of gas, conventionally containing oxygen, is flowed over the sample. TPO is used in applications such as the study of the kinetics of coking, evaluation of carbon burn off, determination of the different forms of carbonaceous deposits present on a catalyst surface after a given reaction involving organic compounds, etc. Coupled TPR/TPO technique offers many advantages. The two techniques can provide useful information in the study of the reactivity and redox behavior of catalysts. The combination of the two reactions of reduction and oxidation represents a real titration of any reducing/oxidant phase by quantification of hydrogen/oxygen consumption.

5.2 Temperature-Programmed Reduction/Oxidation Technique

The developed technique foresees an increase of the sample temperature at a uniform rate ($T_i = T_0 + \beta t$, where β is the rate of temperature increase) measuring and recording the rate at which the sample (or the active component in the sample) reduces/oxidizes under a reducing/oxidizing atmosphere of known concentration. The following reactions hold:

$$\text{TPR: } M_xO_{y(s)} + H_{2(g)} \rightarrow M_{(s)} + H_2O$$
$$\text{TPO: } xM_{(s)} + y/2O_2 \rightarrow M_xO_{y(s)}$$

A typical TPR/TPO apparatus can be assembled following some general principles. The apparatus essentially consists of three parts (i) the gas line for pre-treatments and analysis; (ii) the reactor electrically controlled; (iii) the detector for quantitative evaluation of gas-consumption. At present, all the experimental apparatus used operate at ambient (in flowing gas) or sub-ambient (under vacuum) pressure.

Typically, TCD detectors are mounted (even if many other different types are reported in the literature: detection by pressure changes of the reacting gas, detection by weight change of the solid, etc.), they produced on output signal that is proportional to the concentration of hydrogen or oxygen in the carrier gas. A TC-detector works by measuring the difference in thermal conductivity between the pure carrier gas and the mixture of carrier and reactant gas. For this reason, it is most sensitive when the thermal conductivities of the two gases in mixture are very different. This is why argon or nitrogen are preferentially used as carrier gases in TPR and helium in TPO experiments (thermal conductivities of Ar, N_2, and He of 45.46×10^{-6}, 65.71×10^{-6}, and 376.07×10^{-6} cal/(cm · s · K), respectively and thermal conductivities of H_2 and O_2 of 471.11×10^{-6} and 68.19×10^{-6} cal/(cms K), respectively). Moreover, the change in thermal conductivity is proportional to the mole fraction of reactant gas in the mixture only at low concentrations of reactant gas. To maintain a high detector

sensitivity the concentration of reactant gas in the mixture has to be limited in the 1–10 % range.

When setting a TPR/TPO apparatus (Fig. 5.4), some practical considerations have to be followed. Particular care has to be taken concerning the determination of time/temperature of the reactive events. If the period between the reduction/oxidation of the sample and the detection of hydrogen/oxygen concentration is significantly long, then the measured temperatures (T_{meas}) of the reactive events require correction according to:

$$T_{corr} = T_{meas} - (\beta \cdot V/F) \tag{5.3}$$

where T_{corr} is the corrected temperature, V is the volume between the reactor and detector, and F is the used flow rate. If such corrections are large, the precision of the temperature measurement is reduced and it is advised maintaining high flow rates during experiment. The flow rate must also be compatible with the geometry of the reactor such that the gas flow maintains uniform velocity distribution conditions. Moreover, the flow rate has also to be in relation to the amount of reducible/oxidized sample, as detailed here below.

During the TPR/TPO experiments, several products as H_2O, CO, or CO_2 can be formed. It is important to remove all the undesired gas molecules that can interfere in the signal output. Besides a correct pre-treatment procedure of the sample, use of suitable traps to stop secondary products are necessary and they have to be present in the apparatus configuration.

5.2.1 General Operative Procedure

The procedure to collect TPR/TPO data is also comprehensive of the sample pre-treatment. Several types of procedures can be chosen in relation with the sample nature and type of information required. Generally, before starting a TPR analysis, the sample should be in its oxidized form. In this case, the pretreatment consists in oxidizing the sample in flowing air or pure oxygen and then purging the product formed (like water and carbon residues) by flowing an inert gas. The two procedures have to be carried out at given temperature to assure the effectiveness of the actions. In the case of TPO analysis, the sample has to be previously reduced; in this case too, the reducing procedure has to be carried out at given temperature.

At the beginning of a TPR or TPO experiment, reducing/oxidizing gas is made to flow over a fixed amount of solid at a temperature low enough to prevent reaction. The starting temperature of the experiment has then to be below the expected reduction/oxidation temperature of the phase under study. In this condition, a perfect flat baseline is observed because any hydrogen/oxygen is consumed from the sample (the two branches of TCD are at same concentration of active gas component). Next, the temperature of the sample is increased at a constant rate (β, °C/min) and, as reduction/oxidation begins, hydrogen/oxygen is consumed from the gas mixture (conventionally, H_2/Ar and O_2/He mixtures), which is detected by the detector (TCD).

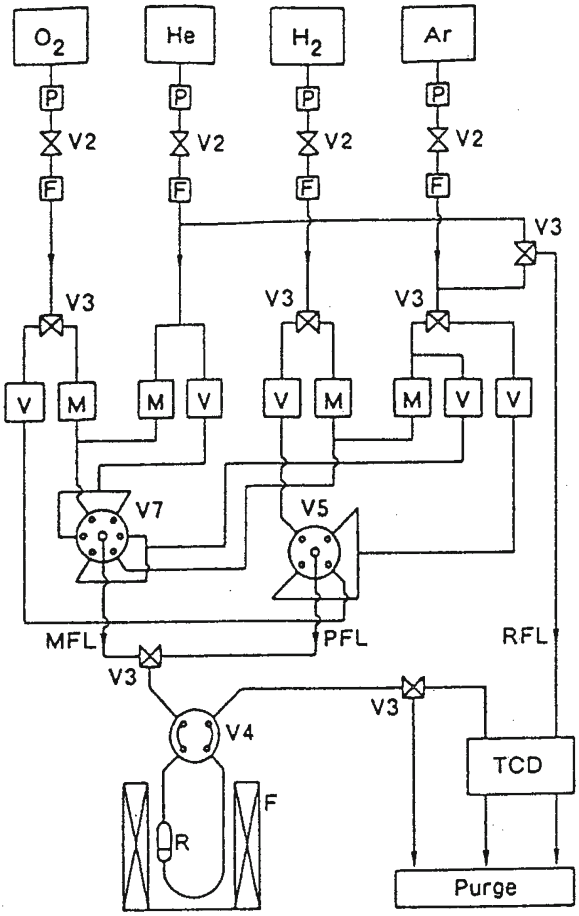

Fig. 5.4 Scheme of a typical TPR/TPO apparatus. Items: *P* pressure controller; *V2* shutoff valve; *F* purification stage; *M* mass flow controller; *V* metering valve; *V3, V5, V7* 3-way, 5-way, and 7-way switching valves, respectively; *V4* crossover valve; *F* temperature controlled furnace; *R* reactor; *PFL* pretreatment flow line; *RFLK* and *MFL* reference and measure flow line of TCD

The TCD signal rises proportionally to the rate of hydrogen/oxygen consumption. When reduction/oxidation ceases, no more hydrogen/oxygen is consumed and the TCD signal returns to its baseline. A peak is obtained (Fig. 5.5) which maximum position represents the maximum rate of hydrogen/oxygen consumed (i.e., temperature of maximum rate of reduction/oxidation, T_{max}). Several peaks ($T_{max,i}$) may be detected over the course of the temperature ramp if different reduction/oxidation steps may occur and each one requires given thermal energy value. The amplitude of each peak is proportional to the reaction rate. On the basis of suitable calibration tests, the amount of consumed hydrogen/oxygen can be obtained from the graphical integration of each peak. Calibration tests are readily achieved by injecting into the

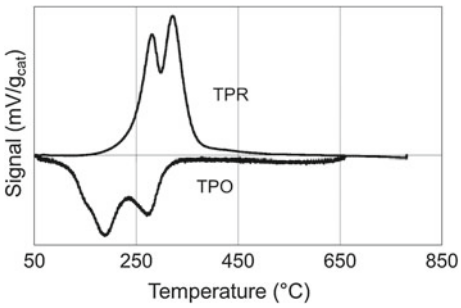

Fig. 5.5 Example of typical TPR and TPO profiles

TPR apparatus known amounts of hydrogen, for example, usually several different amounts. The linear calibration curve obtained (detector signal vs. moles of H_2) is used for the quantitative calculation of the extent of reduction (or oxidation) of the actual sample under study.

5.2.2 Analytical Parameters

The choice of the analytical parameters for a TPR/TPO experiment, in particular sample volume/mass, temperature increasing rate, and flow concentration and flow rate, is fundamental to obtain significant reaction profiles.

Theory predicts that the T_{max} values should be independent of the mass of the sample [8, 9]. Minimal changes in T_{max} were experimentally observed from many authors. The volume (and mass) of the sample is best kept to a minimum as this diminishes problems due to back pressure, temperature differences between sensor and sample, and no uniform gas concentration within the solid. The smaller amount of sample used, it is easier to handle the whole analysis, in particular, less water is formed thus avoiding problems in the water removal system. The main effect of changing the sample mass was that resolution of two separate chemical events obtained with, e.g., 50-mg sample was lost when the sample mass was increased to, e.g., 400 mg with higher value of T_{max} for the composite resultant peak. This behavior is due to the temperature difference between the temperature sensor and the sample that becomes marked for large mass of sample. Therefore, care must be taken in comparing results when sample sizes are markedly different. For example, the two well known rate processes for the reduction of Cu^{2+} to Cu^0 through Cu^+ intermediate, are well distinguished if TPR is performed with low sample mass and low hydrogen concentration [9, 10].

Sample particle size has to be controlled. Particles that are too small can result in the creation of back pressure and consequent problems in maintaining constant flow along the sample, while too large particles can result in intraparticle diffusion problems, causing distorted peaks. Mass transport processes, both inter- and intraparticles, are characterized by low-activation energies and they can thus alter

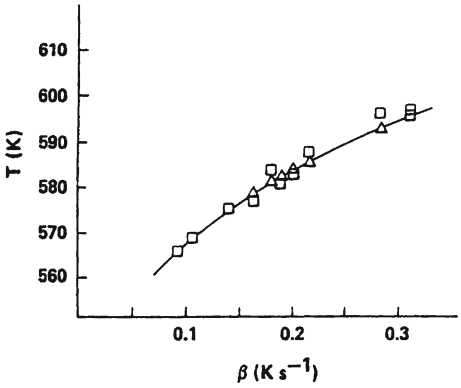

Fig. 5.6 Sensitivity of the temperature of the maximum reduction rate for the reduction process of NiO with β variation

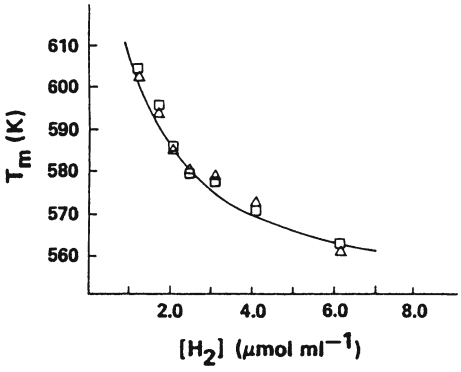

Fig. 5.7 Sensitivity of the temperature of the maximum reduction rate for the reduction process of NiO with H_2 concentration

the shape of reduction profiles. It is common practice to experimentally check for mass transport limitations by looking for changes in TPR/TPO profiles when particle size is varied. Heat transfer limitations can be also considered to be present during reduction/oxidation processes. To avoid or highly limited them, sample dilution with quartz or inert material is commonly performed, this procedure does not alter the TPR/TPO profile.

Concerning the rate of temperature increase, there are advantages in having the heating rate as fast as all the other factors allow. This results in the obtainment of better defined-peaks. Moreover, variation of heating rate (β) leads to variation of T_{max}, this behavior is most commonly used to obtain activation energies for the reactive process. When the change in T_{max} is due to kinetic parameters, other parameters remaining constant, the sensitivity of T_{max} to changes in heating rate is established. For example, systematic study of hydrogen reduction of NiO (simple one-step reduction, from Ni^{2+} to Ni(0), first-order in hydrogen and NiO), showed that an increase in heating rate from 5 to 20 °C/min produced a shift in T_{max} of 30 °C (Fig. 5.6). Exploiting the observed T_{max} with β, activation energy of about 134 kJ/mol was calculated for the NiO reduction process [8].

Concentration of hydrogen/oxygen in TPR/TPO experiment affects the sensitivity of the detector and the T_{max} values vary. For example, an increase on H_2 concentration from 3 % (1.23 μmol/cm^3) to 15 % (6.15 μmol/cm^3) produced a decrease in T_{max} from 330 to 290 °C for the reduction process of NiO [8] (Fig. 5.7). This indicates that the sensitivity is inversely proportional to the H_2 concentration in the reactant mixture.

The variation of the total flow rate influences the results obtained in a TPR/TPO experiment, too. In the case of hydrogen reduction of Cu-exchanged zeolite, an increase in total flow rate from 10 to 20 cm^3/min (with 4 % H_2 concentration) lowered the value of T_{max} by 15−20 °C [9]. Recalling the flow reactor theory, it is expected that an increase in total flow rate for a reactant consumed by a first-order process results in a lowering of the degree of conversion and then an increase of reactant concentration in the reactor. The observed increase of H_2 concentration in the reactor and decrease of T_{max} value of the reduction event with total flow rate are in agreement with theory.

5.2.3 Selection of Operating Parameters

To obtain meaningful TPR/TPO profiles, certain restrictions on the choice of combinations of operating parameters are self-evident. Of particular importance in the case of a TPR experiment, is that the hydrogen feed rate should be equal to the maximum reduction rate, otherwise distortion of the reduction profile will occur. Certain combinations of total flow rate, reactant concentration, sample volume (mass), and heating rate are allowed while other ones are not.

The possibility to carry out a TPR experiment (but the same holds for TPO experiment) with quantitative evaluation of results is based on the simplifying assumption that the mean hydrogen concentration between the reactor inlet and outlet is the driving force for the reduction; that is, the mean hydrogen concentration into the reactor. This holds only if low fractional conversion of hydrogen occurs all along the experiment. On the other hand, the difference of hydrogen concentration between reactor inlet and outlet has to be well detectable, that is, the change in hydrogen concentration has to be large compared to the statistical noise of the detector baseline. Two criteria have to be fulfilled to meet the two requirements above exposed: (i) the amount of hydrogen consumed at the peak maximum should not exceed 2/3 of the hydrogen fed to the reactor and (ii) the minimum conversion at the peak maximum should be 10 %. The two criteria can be met with sets of operating variables. A characteristic number, K (usually expressed in s), has been defined [8] to facilitate the selection of appropriate operating variables:

$$K = S^o/(V^*C^o) \tag{5.4}$$

where V* is the total flow rate of the reducing gas (cm^3/s); S^o, the initial amount of reducible species in the sample (μmol); C^o is the initial concentration of the reducing

gas (μmol/cm^3). The values of K have to be comprised between 55 s and 140 s, with possibility to match S^o, V*, and C^o parameters to obtain the appropriate K value. For values of K below 55 s, the sensitivity of the analysis becomes too low, while for values exceeding 140 s, the amount of reducing gas consumed is too large, so violating the assumption of a linear concentration profile. Concerning the physical meaning of the K parameter, it represents the *sensitivity* parameter. Once optimized K, a second characteristic number can be determined, P (usually expressed in °C), that is defined as:

$$P = K \cdot \beta \tag{5.5}$$

P represents the shape and *resolution* parameter and it has to be comprised between 20 and 50 °C. With the K and P numbers in the correct range, accurate and reliable results from the TPR/TPO analysis and above all comparable data are obtained. The sensitivity of the analysis becomes lower for small heating rates with an inverse proportionality to the hydrogen concentration in the feed. A typical example is in the TPR analysis of CuO: changing the rate of heating and of total flow, two different reaction profiles result. It is possible or not to distinguish the two steps of the reduction process identified by two reducing peaks, Cu(II) → Cu(I) → Cu(0), or to obtain one only peak comprehensive of the total hydrogen consumption involved in the two steps. In the second case, the advantage is to calculate more easily the total amount of the consumed reactive gas. In general, when the sample contains only one component it is useful to perform the analysis with a low temperature rate (b) to observe the mechanism of the reaction process.

5.3 Kinetics and Reduction Mechanisms

The aim of the analysis of the TPR/TPO data is to derive kinetic parameters relating to the reduction/oxidation process. It is common to observe the reduced/oxidized fraction (α) as a function of time for various temperatures and pressures/concentrations of reducing/oxidant gas. The reduction/oxidation of a sample with redox property or of part of it (in the case of supported phase system) is a bulk phenomenon and its degree of reduction/oxidation is interpreted in terms of mechanism by which the reaction occurs. *Nucleation* model or *contracting sphere* model are the most successful utilized kinetic models [2].

In synthesis, at constant temperature, the rate of the reaction: $MO_x + H_2 \rightarrow$ reduced products, may be expressed as:

$$rate = -\mathrm{d}[MO_x]/\mathrm{dt} \text{ or } -\mathrm{d}[H_2]/\mathrm{dt} = \mathrm{k}[H_2]^P[MO_x]^Q \tag{5.6}$$

with P and Q, the reaction orders for the MO_x and H_2 species, respectively.

If the rate constant k is expressed with its dependence on temperature by the classical Arrhenius equation (with A, the pre-exponential factor and E_a, the activation energy) and the linear dependence of temperature on time is introduced by the linear

heating rate ($\beta = dT/dt$), we can write the following expression:

$$-\beta\, d[MO_x]/dT = A\, \exp(-E_a/RT)[H_2]^P[MO_x]^Q \tag{5.7}$$

If the H_2 consumed is little (in accord with the criteria above cited in Sect. 5.2.3, the reaction rate can be considered independent of H_2 concentration and Eq. (5.7) can be rewritten as:

$$-\beta\, d[MO_x]/dT = A\, \exp(-E_a/RT)[MO_x]^Q \tag{5.8}$$

we can now introduce the reduced fraction at given time t (α_t), instead of the residual concentration of sample to be reduced, and being: $\beta\, d(1-\alpha)/dT = \beta\, d(\alpha)/dT$, we can write:

$$\beta\, d(\alpha)/dT = A\, \exp(-E_a/RT)(1-\alpha)^Q \tag{5.9}$$

integration of Eq. (5.9) gives:

$$\int_0^{\alpha} d(\alpha)/(1-\alpha)^Q = A/\beta \int_0^{T} \exp(-E_a/RT)dT \tag{5.10}$$

or

$$\int_0^{\alpha} d(\alpha)/(1-\alpha)^Q = A \int_0^{t} \exp(-E_a/R(T_o + \beta\, t)dt \tag{5.11}$$

with T_o representing the starting temperature of the linear heating rate.

The problem is now to define the correct expression for the variation of α versus t to solve Eq. (5.11) that is to describe the reduction process by a suitable model.

For the derivation of the kinetic parameters of reaction, it is more generally useful to utilize equations able to directly interpret the raw TPR data. Most experimental TPR systems monitor the rate of change of reducing gas concentration as a function of temperature, producing reduction profiles with peaks corresponding to maxima for the reaction rates. Methods originally developed for other temperature-programmed techniques are employed, like thermogravimetry analysis [11–16]. In these approaches, multiple reaction analyses have to be carried out with several different constant heating rates (by varying β), from which the shift of peak maximum position (T_{max}) with β is exploited. The proposed equations converge on linear expressions like that here below recalled, from which both E_a and A can be obtained from the slope and intercept of the relevant line:

$$\ln(T_{max}^2[H_2]/\beta) = E_a/R(1/T_{max}) + \ln(E_a/RA) \tag{5.12}$$

normally, first order kinetics with respect to the reducing sample and hydrogen is assumed and mean hydrogen concentration at the temperature of the maximum reaction rate is considered.

5.3.1 Nucleation Model

When a reducing sample (e.g., oxide) and hydrogen come into contact, the reaction starts and after some time, t_1 (induction time), the first nuclei of the reduced product form. Reduction removes oxygen ions from the lattice and when the concentration of vacancies reached a certain critical value they are annihilated by rearrangement of the lattice with formation of metal nuclei. Oxygen ions may be removed by inward diffusion of hydrogen to the metal/metal-oxide interface or outwards diffusion of oxygen ions from the metal oxide to the metal gas interface. The reaction interface increases more and more rapidly thanks to two processes: (i) the growth of the nuclei already formed and (ii) the appearance of new ones. At a given time of reduction, the metal nuclei have grown at the surface of the oxide grains to such an extent that they begin to make contact with each other. Starting from this moment, a decrease of the reaction interface is observed because of the overlapping of the metal nuclei and the steady consumption of the oxide grains. These processes continue until the complete reduction of the sample; during the final stage in which the reaction interface is shrinking as the reduced layer grows, the process is equivalent to the *contraction sphere* model. The nucleation mechanism results in the S-shaped α against t plot and in the maximum in the $d\alpha/dt$ against α, as illustrated in Fig. 5.8 (left). The same plots are observed for autocatalytic reductions; for example, hydrogen can be dissociated and activated by the reducing oxide; this phenomenon is observed on oxide promoted by metal dopants (doped-CuO and NiO samples).

The mathematical treatment that describes the nucleation mechanism of reduction can be found in Ref. [2]. The final integral equation rate, Eq. 5.13), represents the rising part of the α-vs-t curve before the inflection point (Fig. 5.8 left) and shows that the rate of nucleation is proportional to $(\text{time})^q$:

$$\alpha = \frac{1C_1C_2}{V_{\text{final}}{}^{p+q+1}}(t - t_1)^{q+p+1} \tag{5.13}$$

with C_1 and C_2, proportionality constants; p, the dimension of nuclei; V, the final volume of nuclei; and q, an integer number representing the order of nucleation rate.

5.3.2 Contracting Sphere Model

In many cases, the reaction interface between the oxidized and freshly reduced sample decreases continuously from the beginning of the reaction when it has its maximum value. This can be interpreted in terms of a very rapid nucleation resulting in the total coverage of the reducing grain with a thin layer of the reduced product in the first instant of the reaction. The reaction interface then decreases as the substrate grain is continuously consumed in the course of the reaction. Figure 5.8 (right) shows the contracting sphere model with its decreasing reaction interface resulting in continuously decreasing rate ($d\alpha/dt$ vs. t).

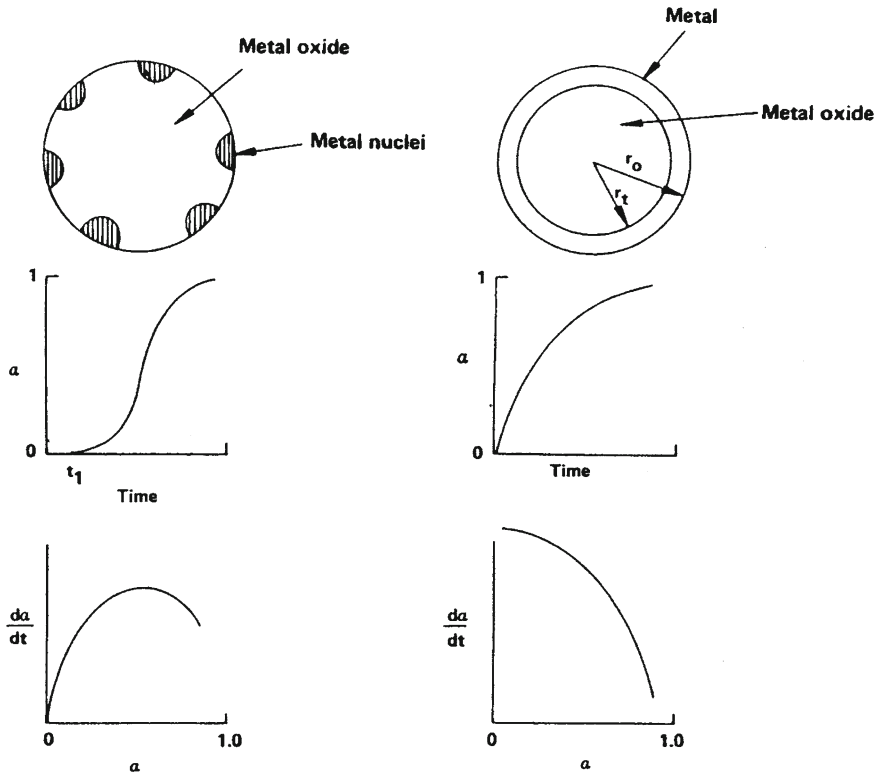

Fig. 5.8 Reduction process by the nucleation mechanism (*left*) and the contracting sphere mechanism (*right*)

The distinction between the nucleation and contracting sphere model is somewhat artificial; in fact the contracting sphere model starts with very rapid nucleation and the nucleation mechanism finishes by an essentially contracting sphere model. The real distinction is between a reaction interface, and reaction rate, that is increasing in the early stages of the reactive process (nucleation model) and a reaction interface that is contracting throughout the reaction (contracting sphere model).

The mathematical treatment that describes the contracting sphere mechanism of reduction can be found in Ref. [2]. The rate of the reaction is controlled by both diffusion from the gas stream to the sample particle and through the reduced layer freshly formed and by chemical reaction at the interface. The final integral equation rate, Eq. (5.14) gives the degree of reduction α as a function of time. The rate constant, k_p, may be higher or lower than the constant rate of hydrogen diffusion, k_d, with the chemical or hydrogen diffusion stage controlling the reaction kinetics, respectively.

$$\frac{k_p}{r_0 d_0}(c_0 - C_{eq})t = [1 - (1-\alpha)^{1/3}] + \frac{r_0 k_p}{k_d}\left[\frac{1}{2} - \frac{\alpha}{3} - (1-\alpha)^{\frac{2}{3}}\right] \qquad (5.14)$$

with C_o and C_{eq}, the hydrogen concentration when reaction rate is zero, r_o, and when it is at equilibrium, respectively; and d_o, the sample density.

5.4 Examples

Typical TPR and TPO analyses of catalysts (bulk, supported, doped, reducing/oxidizing phases) are aimed at evaluating the position of T_{max} peaks and the amount of consumed reducing/oxidizing gas which provides information on (i) easiness to reduction/oxidation; (ii) degree of reduction/oxidation attained; (iii) average oxidation state of given (metal) phases after a given reducing/oxidizing treatment; (iv) dispersion and aggregation state of supported (reducing/oxidizing) phases; *v*) ability to complete a redox cycle.

In the preparation of supported metal catalysts, salt and molecular complex precursors of the metal active components are used; procedures of air-calcination or H_2-reduction are then needed for activating the catalyst for the reaction. Platinum is one among the most important metals widely used as catalytic component for a host of chemical processes. For the preparation of Pt-containing catalysts, the highest Pt-dispersion over suitable supports is highly desirable to avoid the consumption of the costly metal. Therefore, a wide range of platinum compounds have been studied to determine their reduction conditions to obtain the Pt-phase, e.g., $PtCl_4$, H_2PtCl_6, $Pt(NH_3)_2(NO_2)_2$, $Pt(NH_3)_4(OH)_2$, $[Pt(NH_3)_4]Cl_2$, $H_2[Pt(OH)_6]$, ecc. Some Pt-compounds require a four-electron process for reduction ($PtCl_4$, H_2PtCl_6, and $H_2[Pt(OH)_6]$) while the reduction of some others require a two-electron process. The TPR profiles of some dried Pt-samples are shown in Fig. 5.9. It is interesting to note that the Cl-containing salts/complexes are significantly more difficult to reduce than the OH- containing compounds (e.g., in Fig. 5.9 compares the TPR profiles A with B and C; and the D with the E profiles).

In the catalyst preparation, not only the choice of the active phase precursor is crucial, the method of catalyst preparation is decisive, too, for obtaining good dispersion of the active phase. Active phase can be deposited on supports by impregnation, ion-exchange, adsorption, etc. Once selected the nature of support and active phase, the observed differences in dispersion should only be due to the method of preparation. Dispersed iron oxide catalysts (FeO_x) have received much attention because their potentiality for many applications in environmental catalysis (N_2O decomposition and reduction) and in fine chemical industry (Friedel-Crafts, isomerisations, etc.). For most applications, high dispersion of the metal centres is desirable to enhance the activity-selectivity pattern of the catalysts.

Iron oxide is a well reducible phase, the comparison of reduction profiles of supported Fe-catalysts may give information on the dispersion state of iron. In Fig. 5.10, two TPR spectra of two dispersed FeO_x catalysts on zirconia prepared by conventional impregnation and adsorption methods are shown [17]. Reduction of pure hematite (Fe_2O_3) by hydrogen is a complex event that can proceed in different steps

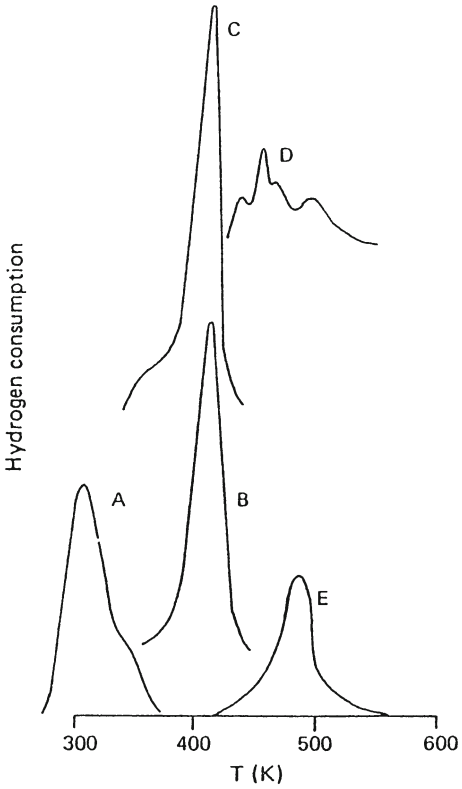

Fig. 5.9 TPR profiles for some Pt salts used in catalyst preparation (from Ref. [2])

via intermediate oxides (i.e., magnetite, Fe_3O_4, and wüstite, FeO_x). The possible reduction reactions, involving hematite, are written here below.

(i) $Fe_2O_3 + 3H_2 \rightarrow 2Fe + 3H_2O$
(ii) $3Fe_2O_3 + H_2 \rightarrow 2Fe_3O_4 + H_2O$
(iii) $3Fe_2O_3 + 3H_2 \rightarrow 6FeO + 3H_2O$
(iv) $Fe_3O_4 + 4H_2 \rightarrow 3Fe + 4H_2O$
(v) $Fe_3O_4 + H_2 \rightarrow 3FeO + H_2O$
(vi) $(1 - x)Fe_3O_4 + (1 - 4x)H_2 \rightarrow 3Fe_(1 - x)O + (1 - 4x)H_2O$
(vii) $FeO + H_2 \rightarrow Fe + H_2O$
(viii) $Fe_(1 - x)O + H_2 \rightarrow (1 - x)Fe + H_2O$

Generally, the first step in the hematite reduction is the formation of Fe_3O_4. Accordingly, observation of a TPR peak at low temperature (the exact position diverges to a large extent dependent on impurities) corresponds to the Fe_3O_4 formation. The Fe_3O_4 reduction profile gave one symmetrical peak with T_{max} at around 550 °C, while the reduction of FeO was observed at very higher temperature (> 750 °C).

A very different and complex situation occurs when supported iron phases are concerned. The TPR profile of the FeO_x/ZrO_2 catalysts prepared by impregnation presents a convoluted curve (Fig. 5.10, left). The complexity of the TPR profile reveals

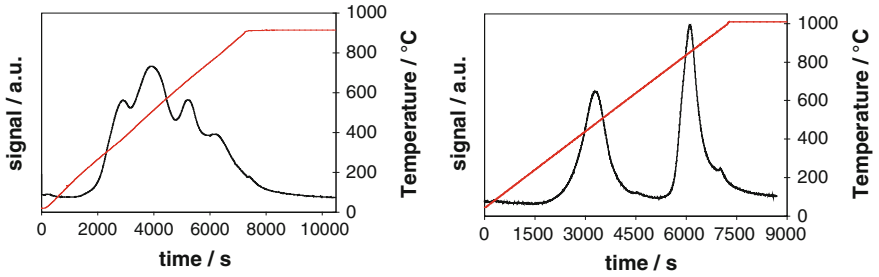

Fig. 5.10 TPR profiles of FeO_x/ZrO_2 (with 5 wt % of Fe) prepared by the impregnation (*left*) and by adsorption equilibrium method (*right*)

the high heterogeneity of the iron surface in terms of nature of the oxide species, dimension of aggregates, and oxide-support interaction. A completely different situation emerges when FeO_x/ZrO_2 was prepared by adsorption method (Fig. 5.10, right). The spectrum is dominated by two well defined and intense peaks positioned at low ($T_{max,1}$at *ca*.430 °C) and high ($T_{max,2}$at *ca*.850 °C) temperature. The two well defined and sharp reduction peaks suggest that iron oxide aggregates are of smaller dimension than those of the impregnated catalyst. The nature of the support can deeply modify the reducing path of the supported Fe_2O_3 phase. Examples can be found in Ref. [18], in which a series of dispersed Fe-catalysts with increasing Fe loading (from 3 to 17 wt.%) has been prepared over a mesoporous silica as support. From a qualitative point of view, all the reducing profiles present the same feature independent of the Fe-content (Fig. 5.11): a main reduction peak with well defined maximum at ca. 400 °C dominates the spectra, other weakly resolved maxima with lower intensity are between 700 and 800 °C. The samples at progressively higher Fe loading consume increasing amount of H_2 without any important modification of the shape and position of the reducing peaks. Concerning the quantitative point of view, the experimental H_2-consumptions are lower than those that can be calculated assuming total reduction of the F_2O_3, assumed as the starting species. It has been determined that the silica matrix had a strong inhibiting effect on the complete Fe(3+) reduction to Fe(0) due to fayalitic phase formation (Fe_2SiO_4). Only the reducible iron oxide aggregates took part in the reaction [18], the high dispersion of the Fe-oxide species imparts acidic- properties of Lewis type to the surface.

The reducibility of any metal oxide can be improved or got worse by doping the oxide. Detailed studies were made on the reducibility of copper oxide. Hurst et al. [2] report an exhaustive study on the CuO phase doped with 2 mol % of a large series of metal ions (Cr, Mn, Fe, Co, Ni, Ru, Rh, Pd, Ag, and Ir, Pt, and Au). The doping with the first-row transition metal ions gives TPR profiles with the same shape as that obtained from CuO with a shift to lower temperatures (293 °C $<$ T_{max} $<$ 313 °C) compared with T_{max} of 333 °C for CuO under the same experimental conditions. The improving effect of these ions on the reducing property of CuO likely arises from nonspecific modification of the CuO lattice, resulting in the increase of copper nucleation sites. The TPR profiles of Pd- and Ru-doped CuO are distinguished from

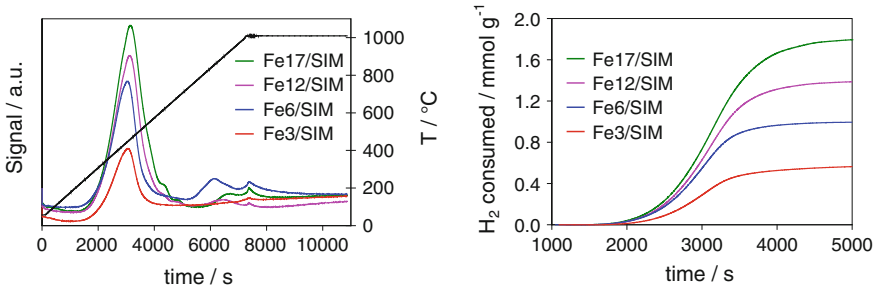

Fig. 5.11 TPR profiles of FeO_x catalysts dispersed on a mesoporous silica (SIM) with different amount of Fe_2O_3, from 3 to 17 wt.% (*left*) and H_2 consumed in the reduction (*right*) (from Ref. [18])

all the others in that reduction is complete at very low temperatures (150−230 °C) and the TPR profiles consist of two peaks which indicate a low-temperature process followed by a more intense high-temperature reduction. Preferential reduction of Pd and Ru ions to form Pd and Ru nucleation sites occurred followed by an improvement of the CuO reducibility. The ion-doping effect of Ag, Au, Rh, Ir, and Pt on CuO is more complex; CuO reduction is completed at about the same temperature as that observed for CuO with a more complex shape of the TPR profile.

The knowledge of the average oxidation state (AOS, $n_{ox,av}$) attained for a given oxide under defined reducing conditions (nature of the reducing agent and temperature, in particular) is of importance for several applications. TPR offers a simple way to compute AOS for any given reducible metal species as an alternative to expensive analytical analyses (i.e., XPS). The simple starting idea is to compare the theoretical amount of electrons needed for the reduction of one mole of species (Ne°_{theor}) with the amount of effective electrons exchanged during reduction (Ne°_{exptl}), obtained from the TPR experiment (derived from the experimental knowledge of H_2 consumed: one mole of H_2 gives 2 electrons during the reduction process). For a mole of reducing species, $n_{ox,av}$ can be calculated as:

$$n_{ox,av} = (Ne^{\circ}_{theor} - Ne^{\circ}_{exptl})/SF \tag{5.15}$$

where SF indicates the stoichiometric factor, number of reducible atoms in the species; for example, SF is 2 for V_2O_5.

In alternative, AOS can be calculated from the balanced redox reaction; here below written for a trivalent metal species, M^{3+}, which can be reduced to bivalent or univalent or zerovalent metal species:

$$M^{3+} + (y-2)/2H_2 = M^{(5-y)+} + (y-2)H^{+} \tag{5.16}$$

where y indicates the experimental amount of hydrogen consumed, obtained from TPR analysis. Once obtained y, the final average oxidation state ($n_{ox,av}$) of M can be calculated on the basis of Eq. (5.16).

Many examples can be found in the literature on this point. The reducibility of vanadia catalysts has catalytic implications for selective oxidation reactions where they found real use. The support nature and the preparation method affect the reducibility of the vanadia phase. In Ref. [19]; pure titania or bilayered titania/silica supports were chosen and concerning the vanadia deposition method, impregnation and atomic layer deposition procedures were performed. The reducibility of vanadia improved with increasing titania loading as shown by the calculated AOS. The lowest AOS were associated to vanadia on pure titania supports ($n_{ox,av} = 3.5$) while vanadia on titania-silica supports achieved at maximum $n_{ox,av}$ of 3.7–3.8. AOS of vanadium after reduction was independent of the preparation method.

When supported metal oxide phases are concerned, the kind of surface species that can be present at the surface depends on the support nature, being active a strong or weak metal-support interaction. CuO is an important catalytic phase, easy to disperse on acid supports that can interact with it with strong metal-support bond; this interaction can influence the redox properties of CuO. Modified silicas with amount of alumina (SA), titania (ST), and zirconia (SZ) in 12–14 wt.% concentration were used to support CuO (8–9 wt.%) [20]; a commercial silica-alumina support was comparatively studied (SAG). On the different supports, the CuO redox properties were controlled by combining TPR and successive TPO experiments.

As depicted in Fig. 5.12, the profiles for the two silico–aluminas (SA and SAG) were well different between each other, in terms of T_{max} values and line widths. For Cu/SAG, two well distinguished peaks of similar intensity and for Cu/SA, four peaks with very different line widths were otained. A set of three peaks described

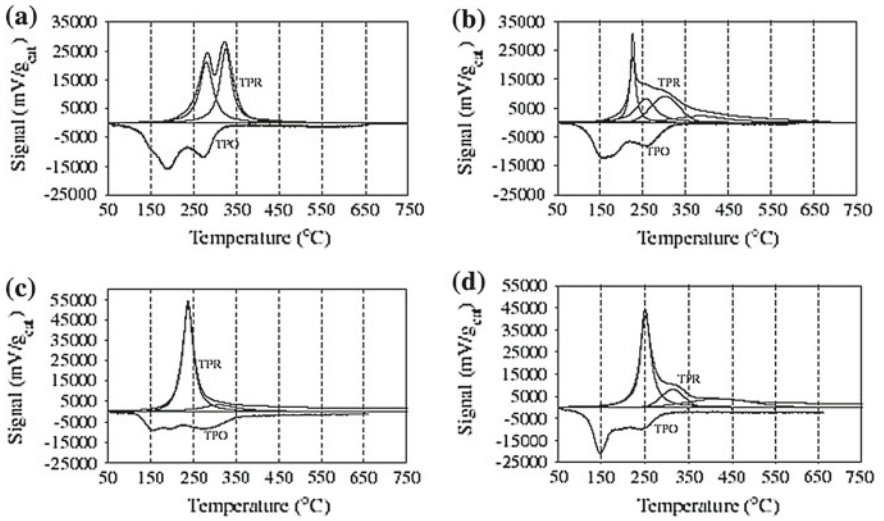

Fig. 5.12 Profiles of reduction (TPR) and oxidation (TPO) at programmed temperature for Cu/SAG (**a**), Cu/SA (**b**), Cu/ST (**c**), and Cu/SZ (**d**). Experimental and decomposed lines are indicated (from Ref. [20])

the TPR profile of Cu/SZ, while quite an unique peak was obtained for Cu/ST. The reduction of the copper phase on the supports of high acidity (SA and SZ) showed low defined and very broadened TPR peaks at very high temperatures, (380−425 °C). The temperature and feature of these peaks suggest that they could be assigned to copper species in interaction with the support. These compounds were more stable to reduction than the dispersed CuO species.

The reoxidation of the reduced copper phase was accomplished by temperature programmed oxydation (TPO). All the studied catalysts could be almost completely reoxidized to CuO, as indicated by the values of oxidation-percent calculated (>60 %). Quite the same TPO profiles were observed on all the catalysts with two oxidation steps: at .first, oxidation of surface copper species and at higher temperature, bulk oxidation. The effective redox properties of CuO allow it to find application in several reaction processes demanding cyclic reduction and reoxidation process with the reactants (i.e., selective catalytic reduction of NO_x with hydrocarbons as reducing agent, [20–22]).

References

1. J. Hu, L. Chen, R. Richards, in *Metal Oxide Catalysis*, vol. 2, ed. by S.D. Jackson, J.S.J. Hargreaves (WILEY-VCH Verlag GmbH & Co. KGaA, Weinheim, 2009)
2. N.W. Hurst, S.J. Gentry, A. Jones, B.D. McNicol, Catal.-Rev.-Sci. Eng. **24**, 233 (1982)
3. R.K. Grasselli, J.D. Burrington, Adv. Catal. **30**, 133 (1981)
4. P. Mars, D.W. van Krevelen, Chem. Eng. Sci. Spec. Suppl. **3**, 41 (1954)
5. A.R. Almeida, J.A. Moulijn, G. Mul, J. Phys. Chem. C. **115**, 1330 (2011)
6. C. Doornkamp, V. Ponec, J. Mol. Catal. A **162**, 19 (2000)
7. B. Jouguet, A. Gervasini, A. Auroux, Chem. Eng. Technol. **18**, 243 (1995)
8. D.A.M. Monti, A. Baiker, J. Catal. **83**, 323 (1983)
9. S.J. Gentry, N.W. Hurst, A. Jones, J. Chem. Soc. Faraday Trans. I, **75**, 1688 (1979)
10. P.A. Jacobs, J.P. Linart, H. Nijs, J.B. Uytterhoeven, J. Chem. Soc. Faraday Trans. I, **73**, 1745 (1977)
11. R.J. Cvetanovic, Y. Amenomiya, Catal. Rev. **16**, 21 (1972)
12. V. Rakic, V. Dondur, D. Misljenovic, J. Therm. Alnal. **38**, 879 (1992)
13. J.H. Chan, S.T. Balke, Polym. Degrad. Stabil. **57**, 135 (1997)
14. P. Carniti, A. Gervasini, Thermochim. Acta **379**, 51 (2001)
15. H. Tanaka, Thermochim. Acta **267**, 29 (1995)
16. F. Eigenmann, M. Maciejewski, A. Baiker, Thermochim. Acta **359**, 131 (2000)
17. C. Messi, P. Carniti, A. Gervasini, J. Thermal Anal. **91**, 93 (2008)
18. A. Gervasini, C. Messi, P. Carniti, A. Ponti, N. Ravasio, F. Zaccheria, J. Catal. **262**, 224 (2009)
19. J. Keranen, P. Carniti, A. Gervasini, E. Iiskola, A. Auroux, L. Niinistö, Catal. Today **91–92**, 67 (2004)
20. S. Bennici, P. Carniti, A. Gervasini, Cat. Lett. **98**, 187 (2004)
21. A. Gervasini, M. Manzoli, G. Martra, A. Ponti, N. Ravasio, L. Sordelli, F. Zaccheria, J. Phys. Chem. B **110**, 7851 (2006)
22. S. Bennici, A. Gervasini, Appl. Catal. B **62**, 336 (2006)